Reflection compensation scheme for the efficient and accurate computation of waveguide discontinuities in photonic crystals

D. Karkashadze, R. Zaridze, A. Bijamov
Laboratory of Applied Electrodynamics, Tbilisi State University
3, Chavchavadze Ave., 380028 Tbilisi, Georgia
e-mail: lae@lae.ictsu.tsu.edu.ge

Ch. Hafner, J. Smajic, D. Erni
Laboratory for Electromagnetic Fields and Microwave Electronics
Swiss Federal Institute of Technology
ETH-Zentrum, Gloriastrasse 35, CH-8092 Zürich, Switzerland
e-mail: christian.hafner@ifh.ee.ethz.ch

***Abstract*—We presented a novel method for the accurate and efficient computation of the reflection and transmission coefficients of waveguide discontinuities within planar photonic crystals (PhCs). This method proposes a novel kind of field source that optimally excites the dominant waveguide mode and mimics procedures that are typically used for the measurement of reflection coefficients. This technique may be applied to arbitrary field simulators working in the frequency domain. The presented reflection compensation scheme is elucidated along the Method of Auxiliary Sources (MAS). In order to verify the results, we compare two test cases with the rigorous connection technique provided by the Multiple Multipole Method (MMP).**

***Indexing Terms*— method of auxiliary sources (MAS), multiple multipole method (MMP), photonic crystals (PhCs), waveguide discontinuities, boundary conditions.**

I. INTRODUCTION

PHOTONIC crystals (PhCs) have first been proposed as an optical counterpart to semiconductor crystals [1], i.e., in PhCs, the photon plays the role of the electron in semiconductors. In nature, PhCs are rarely observed, but nanotechnology allows one to fabricate PhCs as a novel kind of meta-materials. Although it is nice to know that perfect PhCs may exhibit band gaps, i.e., frequency ranges that do not allow electromagnetic waves to penetrate the crystal, this pure meta-material aspect does not sufficiently explain the current interest in PhCs. In fact, doping makes semiconductors attractive and virtually the same holds for PhCs. Despite of this analogy, doping of PhCs is pretty different from the semiconductor doping because the atoms in semiconductors are compared to rather large macroscopic cells of the PhCs. Nanotechnology may allow one to modify any cell of a PhC quite precisely. By introducing linear defects (line of vacancies or substitutional defects with different size or material) into the lattice structure, one can easily obtain waveguide channels in PhCs [2], [3]. One of the main drawbacks of standard waveguides for integrated optics is the fact that the bending radius must be large compared to the wavelength in order to avoid bending loss. This makes standard structures of integrated optics large compared to the wavelength. The PhC concept allows one to obtain sharp waveguide bends virtually without radiation loss and with zero reflection for some distinct frequency [4]-[6] or even for a wide frequency range [7], when some optimization procedure is subsequently added. For the analysis of PhC waveguide bends and PhC waveguide discontinuities, numerical techniques are required that allow one to accurately compute the S-parameters, i.e., the transmission and reflection coefficients at the PhC's waveguide ports. Up to now, a variety of numerical techniques have been proposed [5], [8]-[10].

During the investigation of numerous models for waveguide discontinuities fast and efficient methods are of great interest. This especially holds when the optimization of a whole PhC device is required, such as an achromatic waveguide bend with almost zero reflection over a wide frequency range within the photonic bandgap (PBG) [7]. It has been observed that such optimizations may lead to very critical cells in a PhC [7] that require a highly accurate numerical model. Thus an efficient but highly accurate method is required.

After a short outline of the standard PhC modeling methods and a short introduction to the MMP-connection approach, we present three new procedures 1) for the excitation of the fundamental waveguide modes, 2) for the reflections compensation at the output ports, and 3) for the S-parameters computation. Together with the Method of Auxiliary Sources (MAS) [11] we can apply these procedures to the efficient computation of waveguide discontinuities in PhCs. Comparisons with the rigorous MMP-connection approach demonstrate that the results are sufficiently accurate for being used within optimization procedures.

II. STANDARD PHC MODELING PROCEDURES

In order to obtain a finite-size model for PhC waveguide devices most of the standard procedures truncate the planar PhC structure at some distance *D* from the discontinuity. After this, some fictitious excitation is introduced in order to excite an incident mode at the input port (see Fig. 1). Typically, plane

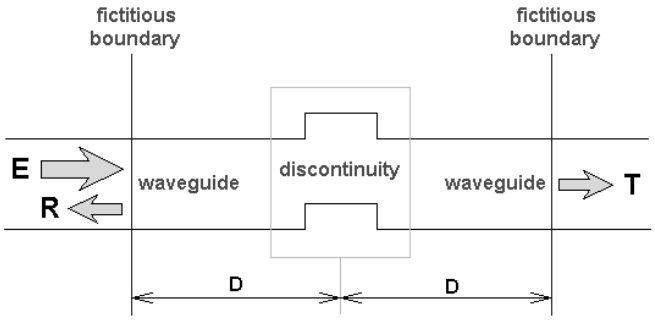

Fig. 1: Schematic treatment of a waveguide discontinuity. The excitation, reflection and transmission of apparent electromagnetic waves are indicated by the corresponding arrows.

waves, monopoles, or dipoles are introduced as fictitious excitations. The proper positioning of the fictitious excitation is crucial because it often happens that a significant amount of the excitation energy does not couple into the desired waveguide mode. Furthermore, the fictitious excitation may also excite higher order or evanescent modes or even additional modes in the output ports. These undesired modes in the output ports can easily be suppressed by using appropriate excitations, i.e. a suitably confined field at the input port. Suppressing the influence of evanescent modes is much more delicate. The distance *D* between the PhC waveguide port and the waveguide discontinuity is limited only by the decay of the evanescent modes produced by the discontinuity itself. Since *D* may extend to large values, the truncated model may also become rather bulky, which leads to long computation times.

An even more difficult problem is imposed by the residual reflections at the output ports. Generally speaking the interface between discrete and continuous translation symmetry (as present in any finite PhC structure) imposes a discontinuity, which causes a bunch of virtually reflected waves that travel back to the discontinuity. Such multiple reflections strongly interfere with a proper estimation of e.g. the S-parameters. The pedestrian way to avoid such undesired reflections at the output ports uses absorbing boundary conditions along the truncation lines (i.e. the fictitious boundary in the Fig. 1). Especially for time-domain methods like FDTD [14], truncation of the infinite space is very straightforward. Thus, many techniques have been developed for absorbing outgoing waves on such boundaries, i.e., at the truncation lines of the finite numerical model. Currently the best technique is PML [15]. Recalling now the special nature of the interface at the PhC boundary where spatial symmetry breaking occurs: Such discontinuity is nearly intractable when using conventional boundary conditions. Therefore, these absorption techniques become very sophisticated, although perfect absorption without any spurious waves is practically impossible.

A laborious way to circumvent the impact of spurious reflections in (time-domain) models relies on time gating, where the distance *D* is increased accordingly to provide a temporal separation between all emergent signal pulses. As a result, such models are either not sufficiently accurate or very time-consuming.

A well-known alternative to the truncated models with fictitious excitation and absorbing boundary conditions is offered by the supercell method that approximates the structure by a periodically continued one [10], [16], [17]. A simple example is given by the W1 defect waveguide (see Fig. 2 for example, where a sequence of point defects is forming the line-defect). The periodic continuation of a waveguide discontinuity is only feasible for relatively simple cases. Furthermore, it is hard to quantify the errors introduced by the periodic continuation, and finally, the supercell method is not efficient at all.

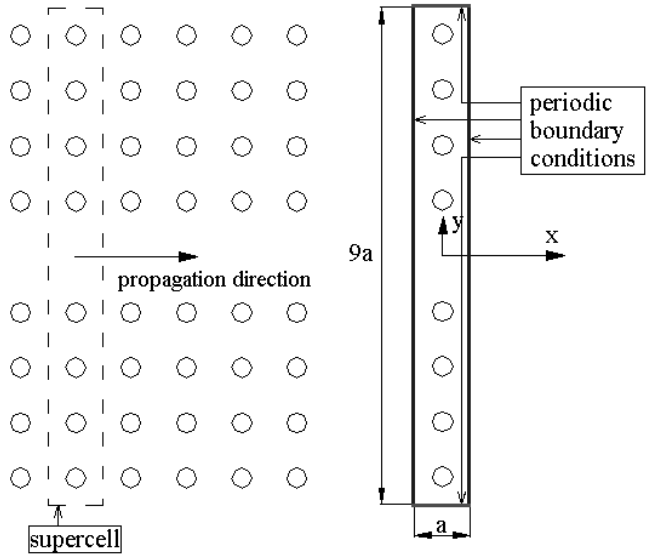

Fig. 2: The supercell approach for a W1 (one line of vacancies) defect waveguide (left). The supercell is defined by its surrounding periodic boundary conditions (right).

III. MMP-Connection Procedure

The most rigorous method for handling waveguide discontinuities in an almost analytic way uses a fictitious separation between the waveguide ports (see Fig. 3) and the area that includes discontinuity [10]. As outlined before along the truncation method, the fictitious separation lines are placed at some distance *D* from the discontinuity. If *D* gets large enough, the evanescent wave amplitude may vanish at the waveguide ports and the fields therein are fully described by the corresponding waveguide's set of guided modes. Along the fictitious separation lines, the modal expansions in the different waveguides are matched with the fields that are excited by the discontinuity region. This is essentially the same procedure as carried out within the standard mode matching technique [18], [19] for the computation of waveguide discontinuities in the microwave regime.

It is worth mentioning that the description of conventional waveguides assumes cylindrical symmetry along the *z*-axis. The longitudinal dependence of the electromagnetic field is then simply described according to

$$\vec{F}\left(\vec{r}_T, z, t\right) = Re\left\{\vec{F}_1\left(\vec{r}_T\right) e^{i(\gamma z - \omega t)}\right\} \tag{1}$$

where a harmonic time-dependence of the form

$$e^{-i\cdot\omega\cdot t} \tag{2}$$

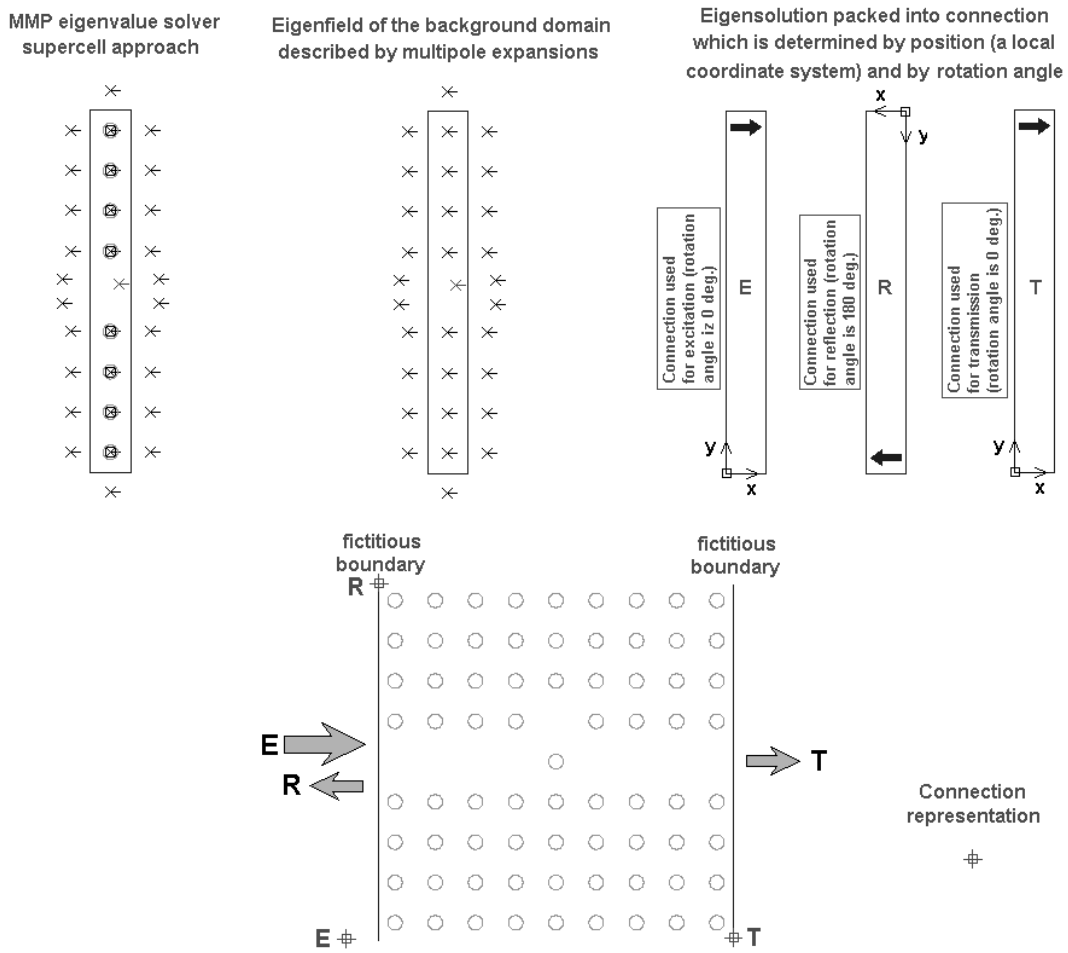

Fig. 3: Schematic description of the MMP-connection procedure: The eigenvalue search is performed as a first step making use of the supercell approach. All information concerning the resulting eigenfield is contained within the set of the waveguide's multipole expansions, which is then packed into a connection. The connection is introduced as a representation of the input (i.e. excitation, E), the reflected (R) and the transmitted (T) electromagnetic wave into the PhC device model.

has been assumed, and the propagation constant γ fully describes the propagation in *z*-direction. Along the direction of propagation, PhC defect waveguides are periodic rather than invariant. Since this is a lower symmetry, the description of the field becomes more complicated. When *x* is assumed as the direction of the PhC waveguide and d_x stands for the periodicity of the PhC in this direction, we have for each mode

$$\vec{F}(\vec{r}+\vec{e}_x d_x) = \vec{F}(\vec{r}) e^{iC_x d_x} \tag{3}$$

where C_x is a complex number that plays the role of the propagation constant. Note that (3) only relates the electromagnetic field at one boundary of the PhC waveguide's unit cell to the field distribution at the opposite boundary (which is separated from the first one by d_x). Thus, C_x does not describe the propagation of the field within the unit cell. Furthermore, if the defect waveguide is confined by two PhC layers that have a finite thickness, in-plane radiation leakage inevitably occurs. This renders C_x to become complex valued even when no material losses are present. The resulting eigenmode analysis gets even more demanding [20], [21], but it does not prevent one from adapting the mode matching technique to PhC waveguides.

The Multiple Multipole Program (MMP) [21] is a very flexible, semi-analytic boundary method that allows one to accurately and efficiently compute not only classical waveguide modes but also the eigenmodes of a PhC waveguide using either the supercell approach or a direct approach that includes radiation leakage as well [20]. In addition the MMP implementation in MaX-1 [22] contains a so-called connection feature. Within this description the data of previously analyzed problem solutions (e.g. the eigenmodes of the PhC waveguide) may be packed into connections that are then introduced as new expansions into the subsequent model of the PhC waveguide discontinuity.

This means that the MMP-connection procedure consists of two different steps: 1) the computation of all relevant modes in the PhC waveguide ports and 2) the computation of the PhC waveguide discontinuity using the modes given by the connections. The former requires the solution of an eigenvalue problem, whereas the latter essentially defines a simple scattering problem.

The main advantages of the MMP-connection scheme are that arbitrary high accuracy and reliability can be reached because of its affinity to mode matching and to analytic procedures. It is important to know that the eigenvalue problem associated with PhC waveguide modes is theoretically demanding, but the resulting matrices set up by the eigenvalue problem are small

because only the unit cell of the waveguide must be taken into account. The scattering model for the PhC discontinuity region is theoretically simpler, but numerically much more demanding because it often involves a larger PhC volume than the waveguide's unit cell, leading to a relatively large matrix equation. Referring to the eigensolutions that are provided as connections we are now able to introduce perfect matching conditions for PhC waveguide terminations. This allows us to significantly reduce the size of the simulation domain, i.e., to decrease the distance *D*. Thus, the resulting MMP matrix becomes relatively small. Consequently not only high accuracy but also short computation times are obtained. Therefore, the procedure is very well suited for any kind of optimization scenario such as the successful optimization of achromatic PhC bends [7] and PhC diplexers [23].

The main drawback of the MMP-connection procedure lays in the fact that the computation of guided modes and its embedding into corresponding connections may become quite demanding. Therefore, only experienced users are able to perform such computations. In the following, we present an alternative technique that does not explicitly requires the PhC waveguide's eigenmodes. For the sake of simplicity only the case of single mode PhC defect waveguides are treated hereafter.

IV. IWGA Sources

The alternative technique relies on the following procedure: Instead of solving an eigenvalue problem for the PhC waveguide's eigenmodes, we now search for a simple, fictitious excitation that mimics the mode profile at the fictitious boundary which accounts for the waveguide termination. In order to emblematize this approach one has just to envision the reciprocal scenario as depicted in Fig. 4 where a radiation field is excited at the termination of a W1 defect waveguide. Just by time-reversing this radiation field one would already get a beam-like excitation for the corresponding PhC waveguide mode.

Even without knowing the proper radiation field as shown in Fig. 4 one may expect efficient waveguide mode excitation while introducing a fictitious but suitably parameterized beam source. First, Gaussian beams [24] may be applied here, but the implementation of an excitation basis that rests on Gaussian beams is still not very straightforward. Furthermore, using complex-origin multipoles [25] or monopoles becomes more natural in the framework of MMP or MAS whereas for the latter only monopoles (i.e., zero order multipoles) are applied (for TM polarization):

$$E_z = A_0 e^{-\mathrm{Im}\{kR_0\}} H_0^{(1)}(kR) e^{-i\omega t}, \tag{4}$$

$$R = \sqrt{\left(x - (x_0 + i\ell\cos\beta)\right)^2 + \left(y - \left(y_0 + i\ell\sin\beta\right)\right)^2}, \tag{5}$$

$$R_0 = \sqrt{\left(x_0 + i\ell\cos\beta\right)^2 + \left(y_0 + i\ell\sin\beta\right)^2}, \tag{6}$$

with $H_0^{(1)}(kR)$ being the zero order Hankel function of the first kind, $A_0 e^{-Im\{kR_0\}}$ is a complex normalizing factor, β stands for the angle of maximal radiation direction, x, y is the observation point, whereas x_0, y_0 defines the source location, ℓ the source half-widths, and for the R and R_0 arguments the principal ones are taken. From Fig. 5 we see that e.g. the modulus of the radiation field E_z provided by the complex origin monopole already gives a good approximation of the fundamental mode at the waveguide termination. Even the scattering field (as given in Fig. 4) is well reproduced by E_z. Hence we call this kind of beam excitation the Imitating WaveGuide Apperture (IWGA) source.

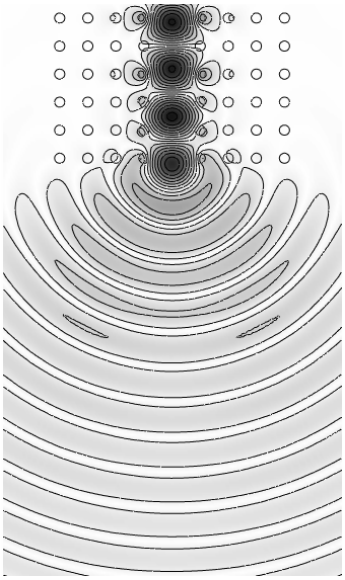

Fig. 4: The E_z-field at a W1 defect waveguide termination.

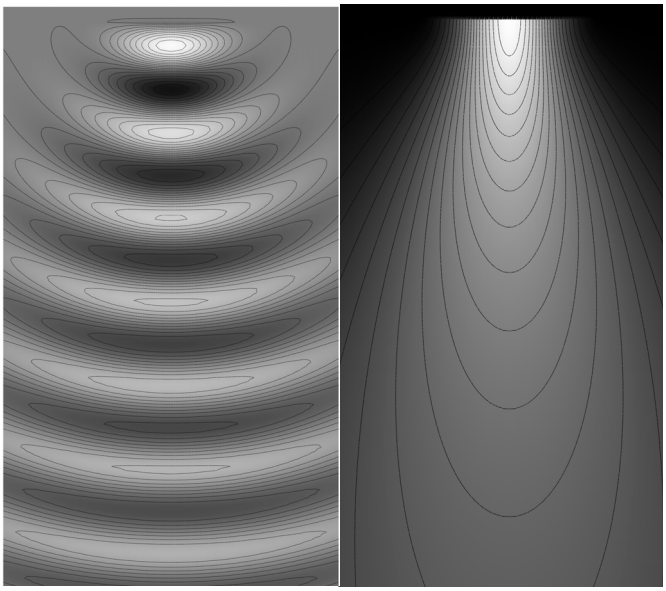

Fig. 5: Intensity plot of E_z (left) and of the modulus of E_z (right) in the *X*-*Y* plane x = [–6.0, 6.0]; y = [–20.5, 0.5]; $x_0 = y_0 = 0.0$; k = 2.0; l = 3.0; β = 270°.

On one hand, finding an appropriate IWGA source is obviously much easier then finding the waveguide's eigenfields by solving a complex eigenvalue problem. On the other hand as the IWGA source may also excite some undesired evanescent modes, the distance *D* associated to the port must be extended compared to the MMP-connection approach where, in principle, evanescent

modes are still tractable. Even if the present version of the proposed technique yet lacks in handling multimode waveguides it is important to see that besides MAS the IWGA source method is also applicable to MMP and all the other frequency domain methods. It should even be possible to develop a time-domain version of this technique.

V. Reflection Extinction at the Output Ports

The IWGA concept essentially handles the excitation problem of the PhC discontinuity in a pragmatic and thus more efficient way than conventional techniques, but it does not solve the problem of the spurious back-reflections at the output ports. This problem is much more demanding. Note that absorbing layers can also be introduced for MMP and MAS but such techniques are difficult and inaccurate for large model sizes. As elucidated earlier the connection concept of MMP removes the reflection problem in a rather rigorous way, but it is difficult to handle. An interesting alternative is obtained from the following consideration.

Given an incident wave, which is transmitted through the waveguide discontinuity and propagates towards one of the output ports. When this mode (which is assumed being fundamental after traveling a sufficient distance in the single-mode defect waveguide) hits the waveguide port (i.e., the boundary of the scattering model associated with the finite PhC structure), it is partially reflected and travels back to the discontinuity (where it is partially reflected again, and so forth). One can now treat the reflected wave at any output port exactly in the same way as the incident wave at the input port. This means one may excite this reflected wave just by setting an IWGA source at the corresponding output port. Assuming a finite PhC structure where a waveguide discontinuity is interconnected to N ports (one input, N–1 outputs), we consider N models consisting of the same scattering model with N different excitations, i.e., N IWGA sources in the N ports. This model is described by a matrix equation with N right hand sides

$$A\, x_{AS} = \left\{ {}^{1}E_z^{inc}\left(x_q, y_q\right),\ {}^{2}E_z^{inc}\left(x_q, y_q\right),\ \ldots,\ {}^{N}E_z^{inc}\left(x_q, y_q\right) \right\} \quad (7)$$

where the matrix A is obtained from the numerical method that handles the discontinuity region, $M(x_q, y_q)$ are the collocation points on the interface surface [21], ${}^{n}E_z^{inc}(x_q, y_q)$ denotes the electric field of the n-th IWGA source (with unit amplitude) placed at the corresponding n-th port.

As an illustrative example (that will be scrutinized later) we analyzed the 90° PhC waveguide bend depicted in Fig. 6 using the MAS [11] simulation code. A standard MAS matrix is obtained 1) when approximating the electromagnetic field in each domain by means of auxiliary sources (i.e., monopolar field expansions), 2) by enforcing simple point matching on the domain boundaries, and 3) making use of an appropriate Tikhonov regularization [26]. The MAS matrix equation (7) is then efficiently solved with LU decomposition techniques. Note that the excitation (i.e. the IWGA source) is contained in the right hand side of the MAS matrix equations. Since we have N IWGA sources, we also obtain N right hand sides. Using LU decomposition the system is solved simultaneously for all N right hand sides, i.e. for all waveguide excitations involved.

The outcome of (7) therefore consists of N field solutions according to the N scattering problems (each having an identical geometry but different excitations). Any superposition of these N fields

$$\begin{aligned} E_z^{total}\left(x, y\right) = \left({}^{1}E_z^{scat} + {}^{1}E_z^{inc} \right) + a_2 \left({}^{2}E_z^{scat} + {}^{2}E_z^{inc} \right) + \ldots \\ + a_N \left({}^{N}E_z^{scat} + {}^{N}E_z^{inc} \right) \end{aligned} \quad (8)$$

is again a solution of the entire problem associated with a linear combination of the corresponding excitations. The linear parameters a_i are then computed in such a way that the amplitude of the incident mode becomes unity whereas the N–1 amplitudes of all reflected waves are forced to vanish. This sets up an additional simple and small system of N–1 equations with regard to the parametrized total field

$$\sum_{n=1}^{N} \int_{L_m^0 - \lambda/16}^{L_m^0 + \lambda/16} \left(E_z^{total}\left(L_m\right) + i\, E_z^{total}\left(L_m + \lambda/4\right) \right) dL_m = 0 \quad (9)$$

Where $m = 1, 2, \ldots, N$ and $2\pi/\lambda = h$ is the propagation constant in the waveguide arm, L_m indicates the centerline of the n-th channel, and L^0_m is its midpoint. In fact (9) defines the matching condition for each PhC waveguide port considering any guided mode involved. Here we just used the spatial shift between real an imaginary part of any traveling wave to be a quarter of a wavelength, which is easily testable by direct substitution of such guided modes into (9). As a result, we obtain the field solution for the waveguide discontinuity but now without any reflections at the output ports

$$\left| E_z^{total}(L_m) \right| = E_m^0 = const\,.$$

The reflection coefficient at the input port and the transmission coefficients for the output ports are computed mimicking the Standing Wave Ratio (SWR) measurement that is well-known from microwave techniques. Thus we define observation lines along the waveguides of the different ports where we compute the total field. Let E^0_m denote the amplitude of the transmitted wave in each output port. The resulting error in fulfilling condition (9) can be determined as follows

$$\frac{1}{L_m} \int_{L_m} \left\| E^{total}(L_m) \right| - E_m^0 \right| \, dL_m = \Delta_m. \quad (10)$$

The amplitudes of the incident and the reflected waves for the input port are determined according to the following standard procedure (for considerable input reflections)

$$\begin{aligned} E_0^{inc} &= \frac{1}{2}\left(\left| E^{total}\left(L_{in}\right) \right|_{\max} + \left| E^{total}\left(L_{in}\right) \right|_{\min} \right) \\ E_0^{reflect} &= \frac{1}{2}\left(\left| E^{total}\left(L_{in}\right) \right|_{\max} - \left| E^{total}\left(L_{in}\right) \right|_{\min} \right) \\ L_{in} &\in \left[L_{in}^0 - \lambda/2,\ L_{in}^0 + \lambda/2 \right] \end{aligned} \quad (11)$$

where L_{in} stands for the input port's centre line, and L^0_{in} for its midpoint. Later it becomes adequate to normalize the electric field in the finite PhC according to E_0^{inc}. For the output ports where the reflection is significantly lower, it is preferable to

determine the transmitted and reflected wave's amplitudes using the relation given below

$$E_{0m}^{transmit} = \frac{1}{L_m}\int_{L_m} \left| E_z^{total}\left(L_m\right)\right| dL_m,$$
$$E_{0m}^{reflected} = \frac{1}{L_m}\int_{L_m} \left| E_{0m}^{transmit} - \left| E_z^{total}\left(L_m\right)\right|\right| dL_m. \quad (12)$$

It should be noted that the evanescent waves being excited at the waveguide discontinuity and at the waveguide ports as well may interfere with the proposed measurement procedure. The waveguide arms must therefore become sufficiently long resulting in a scattering model that is usually larger with respect to the MMP connection approach (but it's still competing well against model sizes required for techniques using imperfect absorbing boundary conditions for the outgoing waves).

In order to illustrate the procedure outlined before, we now consider two simple examples, namely a 90° PhC waveguide bend and a filtering T-junction, which have been previously analyzed along the MMP-connection approach [7], [23].

VI. 90° Bend

Our first test model is a 90° waveguide bend whereas the underlying 2D-PhC consists of dielectric rods arranged in a square lattice and embedded in air. The lattice data are as follows: the radius of each dielectric rod is $r/a = 0.18$ (with $a = 1$ μm being the lattice constant), and the rod's dielectric constant is $\varepsilon = 11.56$. The normalized operation frequency is $a/\lambda = 0.416$. In Fig. 6 the gray rectangle outlines the truncation region of the MAS model. It contains a finite section of 199 rods. Since we know that the PhC structure has a complete band gap only for TM-waves, we only consider *z*-component of the electric field, where *z* is the direction of the cylinder axis. Without lack of generality this considerably simplifies the numerical model.

The electomagnetic field inside each rod is now approximated by a set of M auxiliary sources, i.e., monopoles located on auxiliary lines around the rod. Since the rods are circular, it is reasonable to use a concentric circle as auxiliary line for each rod and to distribute the auxiliary sources uniformly on these circles. Similarly, we introduce a circular auxiliary line inside each rod and uniformly distribute M auxiliary sources for modeling the field outside the rods. Since we are considering the *TM*-polarization, all auxiliary sources are *E*-type monopoles with unit amplitude. Furthermore, we select $M = 12$ being equal for all rods because the rods have the same shape and size. Thus, we obtain a model with $199 \times 2 \times 12 = 4776$ unknowns. These unknowns are then computed by a simple point matching or collocation method on each rod's $M = 12$ uniformly distributed matching points by enforcing there two boundary conditions, namely the continuity for the longitudinal component of the electric field and for the tangential component of the magnetic respectively. As in conventional scattering problems the structure is illuminated by a well-defined incident wave. In our case the IWGA sources are located in the center of both input and output ports as shown in Fig. 6. Thus, we obtain a linear system of 4776 equations with 4776 unknowns and two right hand sides. The computation time for this problem on an Athlon 1200 PC is approximately 180 seconds when using the LAPACK LU-decomposition routine for the matrix solution.

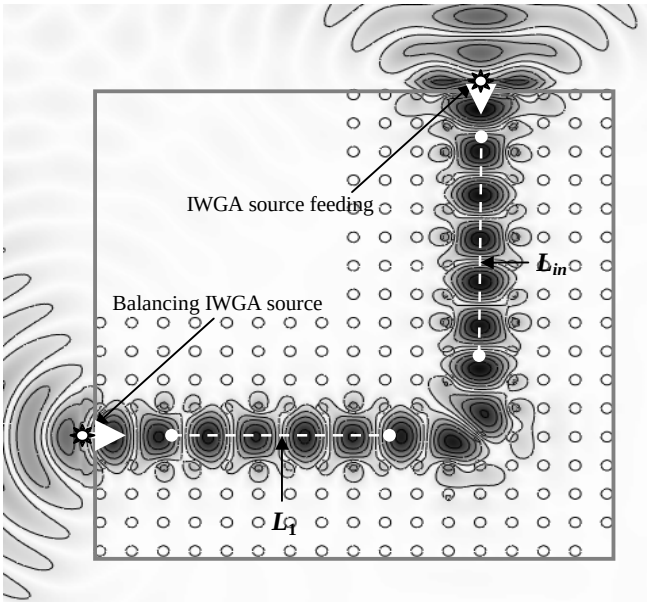

Fig. 6: MAS simulation of the 90° W1 defect waveguide bend. The gray rectangle outlines the truncation boundary of the finite PhC model. The underlying PhC consists of a square lattice with $a/\lambda = 0.416$, $\varepsilon = 11.56$, and $r/a = 0.18$.

(i) MAS simulation; relative error of *E* and *H*: 0.3%; Transmission $T_1 = 91.15\%$; Reflection $R_{in} = 8.58\%$.

(ii) MMP simulation; relative error of *E* and *H*: 0.45%; Transmission $T_1 = 91.26\%$; Reflection $R_{in} = = 8.56\%$.

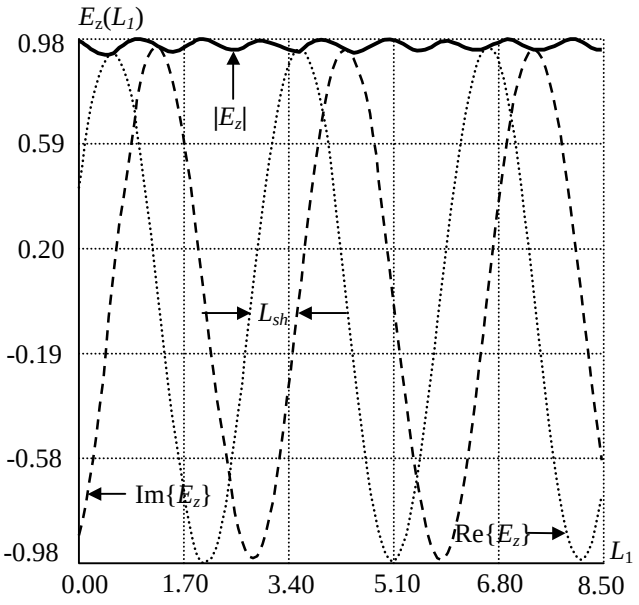

Fig. 7: Electric field E_z along the line L_1. At the low SWR value in the waveguide arm the L_{sh}-value (i.e. the phase-shift between Re{E_z} and Im{E_z}) determine the propagation coefficient: $h = 2\pi/(4L_{sh})$.

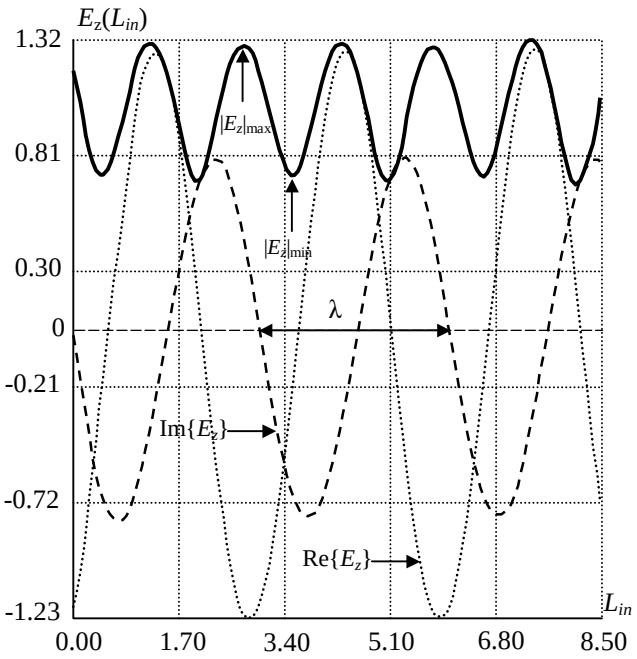

Fig. 8: Electric field along the line L_{in} in input port. The propagation constant is $h = 2\pi/\lambda = 2.068$ and the amplitude of the reflected wave $E_0^{reflect} = ½(|E_z|_{max} - |E_z|_{min}) = 0.2928$; thus, power reflection becomes $R_{in} = (E_0^{reflect})^2 100\% = 8.58\%$.

As soon as the linear system for the two right hand sides is solved the superposition of the corresponding two solutions is computed in such a way that the reflected wave at e.g. the output port (or the reflected field in the horizontal arm) vanishes.

Fig. 7 shows the resulting dependence of the electric field along the observation line L_1 in the center of the horizontal arm (as defined in Fig. 6). It is clearly visible, that this function shows some oscillatory behavior (instead of being constant) due to inaccuracies in the matching procedure at the output port. It is reasonable to assume that the amplitude of the transmitted wave lays somewhere between the maximum and minimum of the oscillating envelope. We therefore define power transmission according to the mean $|E_z|$ value along L_1:

$$E_{01}^{transmit} = \frac{1}{L_1}\int_{L_1} \left|E_z^{total}(L_1)\right| dL_1 = 0.9547; \qquad (13)$$

$$T_1 = \left(E_{01}^{transmit}\right)^2 100\% = 91.15\%,$$

Furthermore, the mean $|E_z|$ deviation form the average value (i.e. the difference between the maximum and minimum value)

$$\Delta_1 = \frac{1}{L_1}\int_{L_1} \left|E_{01}^{transmit} - \left|E_z^{total}(L_1)\right|\right| dL_1 = 0.01 \qquad (14)$$

gives us some information about the accuracy of reflection suppression in the output ports with regard to our MAS simulation scenario. Fig. 8 shows the behavior of the electric field in the vertical arm, i.e. near the input port. As one can see this mimics a nice standing wave pattern from which one can not only obtain the reflection coefficient but also an approximation of the propagation constant, or more precisely of the guided mode's

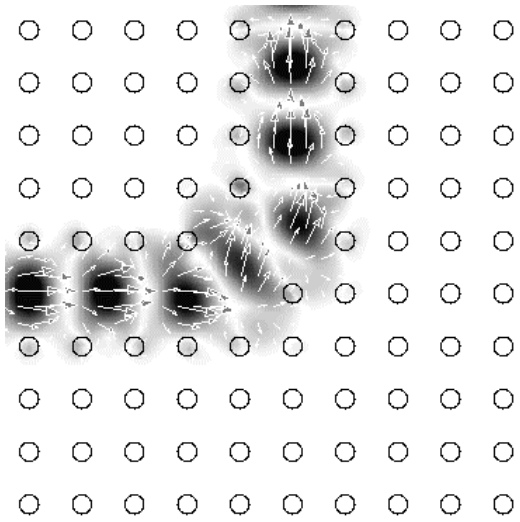

Fig. 9: Poynting vector field distribution within the 90° W1 defect wave-guide bend achieved with MMP. The model data are the same as in Fig. 6.

characteristic constant C as given e.g. in equation (3). It is easy to understand that C is complex valued due to the inplane radiation leakage [20] of the waveguide but since these losses are usually extremely small C becomes almost real.

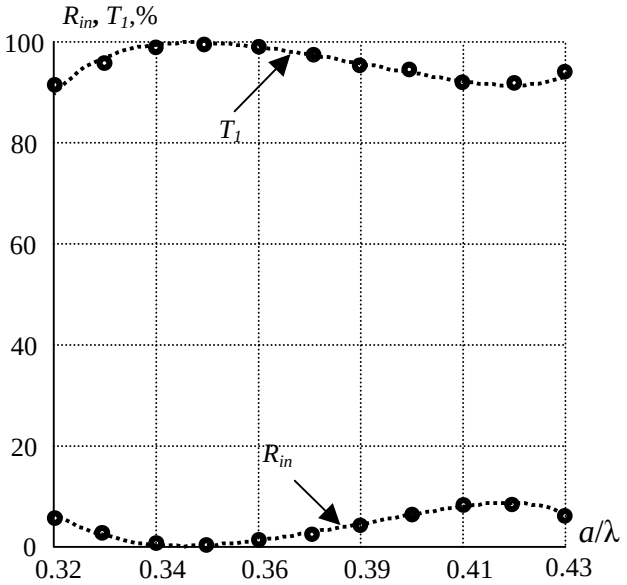

Fig. 10: Comparison of the MAS (circles) and MMP (dashed lines) model for a 90° W1 defect wave-guide bend as a function of the normalized frequency a/λ. The discrepancy is less than 1%.

In addition to the error estimated for the reflection suppression, we can also consider energy conservation. Neglecting radiation leakage we obtain $T_1 + R_{in} \approx 91.15\% + 8.58\% = 99.73\%$. These internal error checks already show an acceptable accuracy of the proposed MAS model. In order to obtain even more information on the quality, we compare these results with those of a model based on MMP-connections. The comparison is

visualized in Fig. 10.

As one can see from e.g. Fig. 6 and Fig. 9, the MMP model is considerably smaller and consists of only 89 rods. Here, the field inside each rod is approximated by a Bessel-type expansion whereas the field outside is represented by a multipole expansion. The total number of unknowns per rod is 22, that is almost the same as in the MAS model. Thus, we only have $22 \times 89 = 1958$ unknowns, i.e., less then half of what we have for the MAS model. But now, the handling of the output ports with connections requires the introduction of a fictitious boundary that separates the region of the PhC discontinuity from the PhC waveguide problem. Along these fictitious boundaries, additional multipoles must be placed together with the connections that describe the waveguide

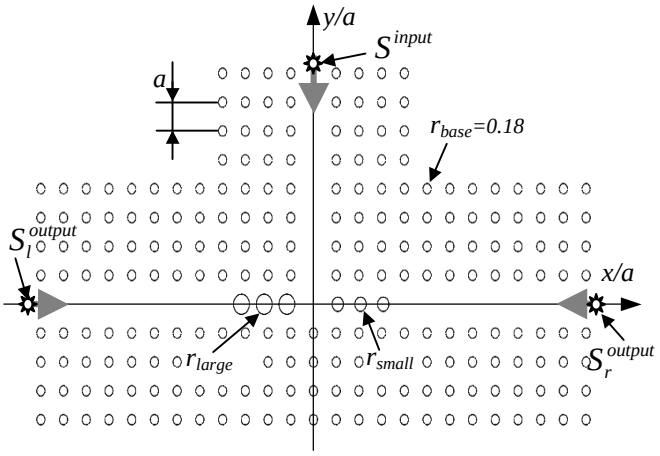

Fig. 11: Geometry of the filtering T-Junction (diplexer).The radii of the rods are given in units of lattice the period *a*. For all of rods: $\mu = 1.0$; $\varepsilon = 11.56$.

modes. Finding an appropriate set of matching points for the resulting model is rather difficult. In order to overcome these problems, MMP works with a generalized point matching technique that leads to an overdetermined system of equations which is then solved in the least squares sense. In our example, we obtain 2181 unknowns for 8964 matching conditions. The solution of this system involves the QR decomposition routine of LAPACK and takes 177 seconds, i.e., almost the same computation time as the MAS solution. Note that the MMP system of equations is more than four times overdetermined. Usually two times overdetermined systems are still sufficient and in our special case, we could use even no overdetermination for the PhC lattice (i.e. the rods) and an overdetermination factor two for the fictitious boundaries. This would allow us to reduce the computation time of the MMP-connection model by a factor of three. Since this model serves only for comparison purposes and because the minimization of the computation time in the framework of MMP could become quite tricky, we did not optimized the model with regard to speed-up.

Fig. 10 shows the comparison of MAS and MMP results where we can see an excellent agreement between these two results. Furthermore, we observe our error estimation to be quite reliable. In conclusion, the simulation of complicated PhC waveguide discontinuities is now reduced to the solution of a standard scattering problem.

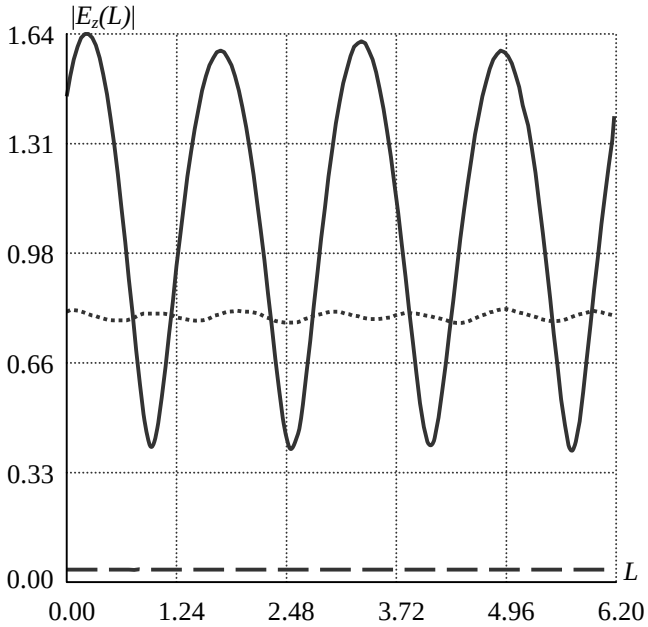

Fig. 12: Distribution of $|E_z|$ along the test lines at $f = 1.23 \cdot 10^{14}$ Hz: —— vertical arm; – – – – left arm; ····· right arm

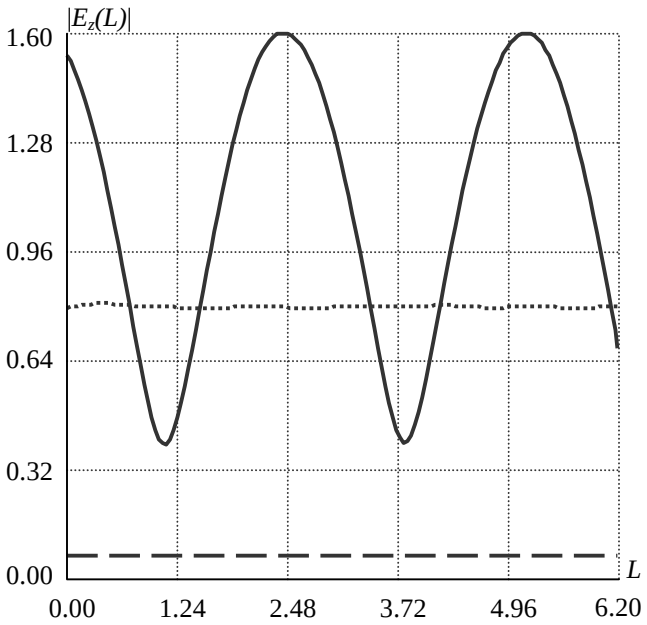

Fig. 13: Distribution of $|E_z|$ along the test lines at $f = 1.038 \cdot 10^{14}$ Hz: —— vertical arm; – – – – right arm; ····· left arm

VII. Filtering T-Junction

The analysis of filtering T-junction as depicted in Fig. 11 is more demanding than the 90° PhC waveguide bend for several reasons. First of all, it has two output ports where the incoming wave is guided to the left output port at an operating frequency of $f = 1.038 \cdot 10^{14}$ Hz and to the right output port for $f = 1.23 \cdot 10^{14}$ Hz. Within our analysis we must evaluate this model at least for two different frequencies, i.e., the computation time is doubled.

Furthermore, wavelength selective power splitting is enabled,

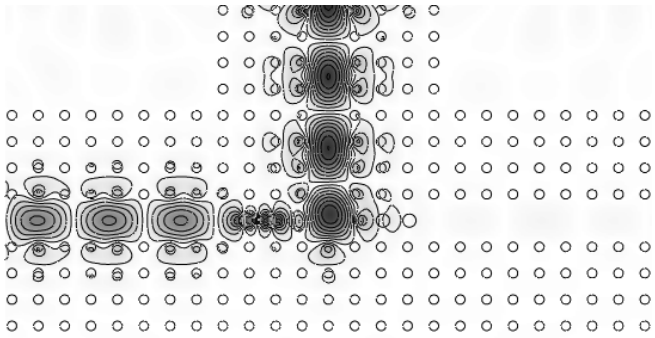

Fig. 14: MAS analysis: E_z-field of the filtering T-junction at $f = 1.038 \cdot 10^{14}$ Hz.

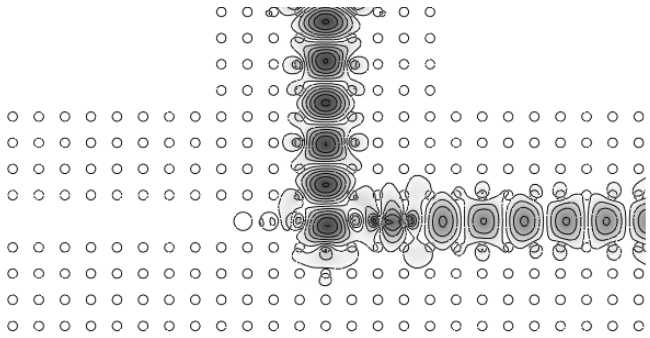

Fig. 15: MAS analysis: E_z-field of the filtering T-junction at $f = 1.23 \cdot 10^{14}$ Hz.

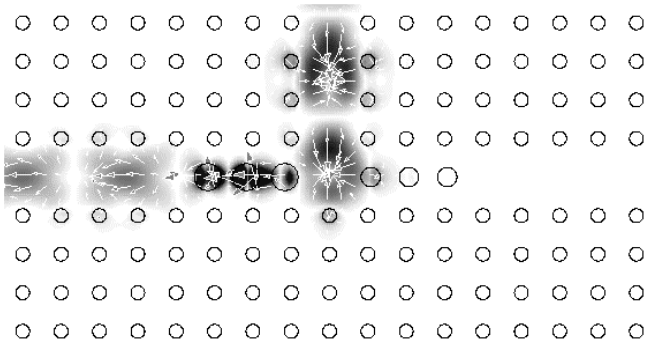

Fig. 16: MMP analysis: Poynting vector field distribution within the filtering T-junction at $f = 1.038 \cdot 10^{14}$ Hz (left diplexer channel).

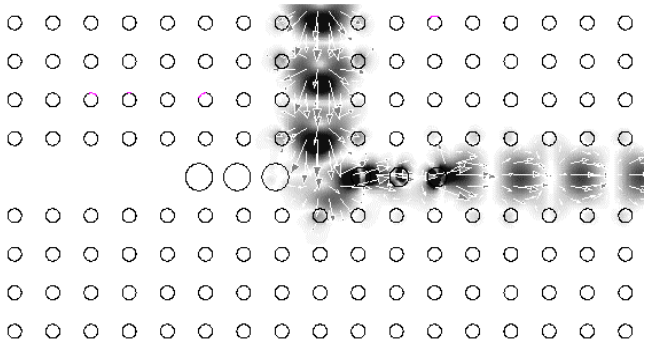

Fig. 17: MMP analysis: Poynting vector field distribution within the filtering T-junction at $f = 1.23 \cdot 10^{14}$ Hz (right diplexer channel).

by introducing corresponding dispersive elements (like e.g. substitutional defects) into the two output waveguides of the T-junction. Such substitutional defects may consist of rods with different sizes compared to those of the underlying PhC lattice

$$r_{base} = 0.18; \quad r_{large} = 0.35; \quad r_{small} = 0.25.$$

The numbers of auxiliary sources and matching points for these rods are slightly higher (we use $M = 14$ for the rods that constitute the PhC lattice and $M_f = 16$ for the substituitional defects).

The MAS model is described here by a matrix equation, which contains 6576 equations with 6576 unknowns and three right hand sides due to the existence of one auxiliary IWGA source per port (see Table 1).

Table 1

Source	x_0	y_0	β	l
Input	0.0	8.5a	270º	3.5a
Left	-12.5a	0.0	0º	3.5a
Right	12.5a	0.0	180º	3.5a

The unknown amplitudes of the IWGA sources are determined according to condition (9), i.e. the reflections suppression condition at the cutoff slice $x_0 = \pm (12 \cdot a + r_{base})$. We shall not care about the matching condition at the input port $y_0 = 8 \cdot a + r_{base}$ because there is always a reflected wave present coming from the discontinuity (i.e. branching region) itself.

Table 2

	$f = 1.038 \cdot 10^{14}$ Hz		$f = 1.23 \cdot 10^{14}$ Hz	
Source	$\lvert A_0 \rvert$	Phase	$\lvert A_0 \rvert$	Phase
Input	1.0	0°	1.0	0°
Left	0.2774	-35.4°	0.0058°	-75.0°
Right	0.0232	-22.1°	0.1370°	-20.7°

This wave will impact the incoming field accordingly but its influence is minimized when using the input field amplitude as normalization for all other wave amplitudes involved. In all other respects the procedure is the same as for the 90° PhC waveguide bend. The solution of the excitation problem (7) and the reflection suppression condition (9) for the given T-junction (Fig. 11) provide one with the values for the complex IWGA sources' amplitudes (Table 2). Since we now dispose of the IWGA source amplitudes (and phase values) providing efficient wave matching at the output ports, we obtain almost constant field distributions along the two observation lines in the output arms of the T-Junction for the two different frequencies (see Fig. 12 and 13).

Table 3

$f = 1.038 \cdot 10^{14}$ Hz, $h = 2\pi/\lambda = 1.156$					
Port	$\lvert E^{trans} \rvert$	$T(\%)$	$\lvert E^{reflect} \rvert$	$R(\%)$	SWR
Input	1.0	100	0. 6031	36.38	2.144
Left	0.7982	63.71	0.0024	0.001	1.000
Right	0.0652	0.42	0.0002	0.000	1.000

Table 4

Case	MMP solution				MAS solutions			
	R (%)	T_l (%)	T_r (%)	Σ (%)	R (%)	T_l (%)	T_r (%)	Σ (%)
Left	35.37	63.38	0.41	99.16	36.38	63.71	0.42	100.51
Right	36.51	0.11	63.24	99.86	36.02	0.11	63.76	99.89

Knowing the field distribution in the two output channels the transmission/reflection coefficients, the propagation constants and a first estimate of the error can be obtained using equations (9)-(12):

a) Propagation constant: $h = 2\pi/\lambda = 2.00$

b) Amplitude of the reflected wave in the output port

$$E_{in}^{reflect} = \frac{1}{2}\left(\left|E_z\left(L_{in}\right)\right|_{\max} - \left|E_z\left(L_{in}\right)\right|_{\min}\right) = 0.6002,$$

the corresponding power reflection coefficient and the SWR

$$R_{in} = \left(E_{in}^{reflect}\right)^2 \cdot 100\% = 36.02\%,$$

$$SWR = \frac{1+\left(E_{in}^{reflect}\right)^2}{1-\left(E_{in}^{reflect}\right)^2} = 2.125, \quad E_{in}^{trans} = 1.0;$$

c) Amplitude of the transmitted wave in the right arm

$$E_{right}^{transmit} = \frac{1}{L_{right}} \int_{L_{right}} \left|E_z^{total}\left(L_{right}\right)\right| dL_{right} = 0.7985,$$

and the corresponding transmission coefficient

$$T_{right} = \left(E_{right}^{transmit}\right)^2 100\% = 63.76\%;$$

d) Amplitude of the reflected wave from the end of the right arm

$$E_{right}^{reflected} = \frac{1}{L_{right}} \int_{L_{right}} \left|E_{right}^{transmit} - \left|E_z^{total}\left(L_{right}\right)\right|\right| dL_{right} = 0.0075,$$

and the corresponding standing wave ratio $SWR = 1.002$;

e) Amplitude of the transmitted wave in the left arm

$$E_{left}^{transmit} = \frac{1}{L_{left}} \int_{L_{left}} \left|E_z^{total}\left(L_{left}\right)\right| dL_{left} = 0.0335,$$

and the corresponding transmission coefficient

$$T_{left} = \left(E_{0left}^{transmit}\right)^2 100\% = 0.11\%;$$

f) Amplitude of the reflected wave from the end of the left arm

$$E_{left}^{reflected} = 0.0003,$$

and corresponding standing wave ratio is $SWR = 1.002$.

g) Energy balance: $\Delta W = T_{in} - (R_{in} + T_{left} + T_{right}) = 0.1\%$

The solution of the initial boundary problem provides the continuity of the *E*- and *H*-field components along the boundary with the error of less than 0.1% Having such high precision of the calculation allows detailed investigation of the wave propagation characteristics in complicated finite PhC. For example Fig. 14 and Fig. 15 show the contour plot of the electromagnetic field component E_z for the given diplexer geometry. The calculated amplitude of the electric field along the each waveguide channel for a frequency of $f = 1.038 \cdot 10^{14}$ Hz is depicted in Fig. 13 whereas the transmission/reflection coefficients are listed in Table 3.

The overall simulation procedure and the degree of accuracy is comparable to the analyis of the 90° PhC waveguide bend. As shown in Fig. 14 and Fig. 15 accurate calculations allow a very detailed description of the complicated fields in finite PhC devices. In order to compare the results with MMP, we use a MMP-connection model (see Fig 16 and 17) that sets up an over-determined 2974×9126 matrix and requires almost the same computation time as the corresponding MAS-model. Comparable figures that result from the two methods are listed in Table 4. As one can see, there is an excellent agreement between both methods.

VIII. Conclusions

We have presented a new powerful method for the accurate and efficient computation of PhC waveguide discontinuities. The method essentially proposes (i) the introduction of special IWGA sources that excite the guided modes in the PhC waveguides and (ii) it provides also a very straightforward technique for suppressing reflected waves at the waveguide ports. Together with such excitation and matching conditions the method delivers an additional technique for the computation of the S-parameters in PhC devices. This rather intuitive way (i.e. when relying on the minimization of the SWR) will gain recognition especially when complicated waveguide structures in e.g. planar 3D-PhCs are involved and thus proper eigenmode calculation becomes too cumbersome. Even if the proposed technique was developed for the method of auxiliary sources (MAS) it will easily apply for any other frequency domain method.

IX. Acknowledgement

This work was supported by the Swiss National Science Foundation in the framework of project NFP-SCOPES-7GEPJ065551 and the research initiative NCCR Quantum Photonic.

References

[1] E. Yablanovich, “Inhibited spontaneous emission in solid-state physics and electronics”, *Phys. Rev. Lett.*, 58, pp. 2059-2062, 1987.

[2] E. Centeno, D. Felbacq, “Guiding waves with photonic crystals,” *Opt. Commun.* 160, pp. 57-60, 1999.

[3] H. Benisty, “Modal analysis of optical guides with two-dimensional photonic band-gap boundaries,” *J. Appl. Phys.* 79, pp.7483-7492, 1996.

[4] R. D. Meade, A. Devenyi, J. D. Joannopoulos, O. L. Alerhand, D. A. Smith, K. Kash, “Novel applications of photonic band gap materials: Low-loss bends and high Q cavities,” *J. Appl. Phys.* 75, pp. 4753-4755, 1994.

[5] A. Mekis, J. C. Chen, I. Kurland, S. Fan, P. R. Villeneuve, J. D. Joannopoulos, “High transmission through sharp

bends in photonic crystal waveguides," *Phys. Rev. Lett.* 77, pp. 3787-3790, 1996.

[6] A. Chutinan, M. Okano, S. Noda, "Wider bandwidth with high transmission through waveguide bends in two-dimensional photonic crystal slabs," *Appl. Phys. Lett.* 80, pp. 1698-1700, 2002.

[7] J. Smajic, Ch. Hafner, D. Erni, "Design and optimization of an achromatic photonic crystal bend", *Opt. Express* 11, 1378-1384,2003, http://www.opticsexpress.org/abstract.cfm?URI=OPEX-11-12-1378 .

[8] M. Koshiba, Y. Tsui, M. Hikari, "Time-domain beam propagation method and its application to photonic crystal circuits," *J. Lightwave Technol.* LT18, pp. 102-110, 2000.

[9] J. Yonekura, M. Ikeda, T. Baba, "Analysis of finite 2-D photonic crystals of columns and lightwave devices using the scattering matrix method," *J. Lightwave Technol.* LT17, pp. 1500-1508, 1999.

[10] E. Moreno, D. Erni, Ch. Hafner, "Modeling of discontinuities in photonic crystal waveguides with the multiple multipole method," *Phys. Rev. E* 66, 036618, 2002.

[11] F. G. Bogdanov, D. D. Karkashadze, and R. S. Zaridze, in "Generalized Multipole Techniques for Electromagnetic and Light Scattering", edited by T. Wriedt, pp. 143-172, Elsevier, Amsterdam, 1999.

[12] A. Bijamov, I. Paroshina, D. Karkashadze, Simulation of optical control devices based on photonic band structures. Proceedings of the Seminar/ Workshop "Numerical Solution of Direct and Inverse Problems of the Electromagnetic and Acoustic Waves Theory, DIPED-2003, 2003.

[13] D.D.Karkashadze, F.G.Bogdanov, R.S.Zaridze, A.Y.Bijamov, C.Hafner, and D.Erni. "Simulation of Finite Photonic Crystals Made of Biisotropic or Chiral Material. Using the Method of Auxiliary Sources". Advances in Electromagnetics of Complex Media and Metamaterials. Edited by Said Zouhdi, Ari Sihvola and Mohamed Arsalane, NATO Science Series. II Mathematics, Physics and Chemistry - Vol. 89, pp. 175-193, 2003.

[14] K. S. Yee, "Numerical solution of initial boundary value problems involving Maxwell's equations in isotropic media," *IEEE Trans. Antennas Propagat.*, vol. AP-14, pp. 302-307, 1966.

[15] J. P. Berenger, "A perfectly matched layer for the absorption of electro-magnetic waves, " *J. Comp. Phy.* 114, pp. 185-200, 1994.

[16] K. Sakoda, *Optical Properties of Photonic Crystals*, Springer, Berlin, 2001.

[17] J. D. Joannopoulos, R. D. Meade, J. N. Winn, *Molding the Flow of Light*, Princeton University Press, 1995.

[18] A. Wexler, "Solution of waveguide discontinuities by modal analysis," *IEEE Trans. On Microwave Theory and Techniques*, Vol. MTT-15, pp. 508-517, 1967.

[19] R. Sorrentino, *Numerical methods for passive microwave and milimeter-wave structures*, IEEE Press, Ch. 8, New York, 1989.

[20] K. Rauscher, J. Smajic, D. Erni, and Ch. Hafner "The open-supercell approach for the eigenmode analysis of 2-D photonic crystal defect waveguides," submitted to *Phys. Rev. E*., 2003.

[21] Ch. Hafner, *Post-modern Electromagnetics Using Intelligent MaXwell Solvers*, John Wiley & Sons, 1999.

[22] Ch. Hafner, MaX-*1: A visual electromagnetics platform*, John Wiley & Sons, 1998.

[23] J. Smajic, Ch. Hafner, D. Erni, "On the design of photonic crystal multi-plexers", *Opt. Express* 11, pp. 566-571, 2003, http://www.opticsexpress.org/abstract.cfm?URI=OPEX-11-6-566 .

[24] G. A. Deschamps, "Gaussian Beams as a Bundle of Complex Rays", *Electron. Lett.* 7, pp. 684-685, 1971.

[25] A. Boag, R. Mittra, "Complex Multipole Beam Approach to 3D Electro-magnetic Scattering Problems", *J. Opt. Soc. Am. A*, Vol. 11, pp. 1505-1512, 1994.

[26] A. Tikhonov, V. Arsenin, *Solutions of ill-posed problems*, Winston and Sons., Washington DC, 1977.

Christian Hafner was born in Zurich, Switzerland, in 1952. He received a Dipl. El.-Ing. Degree, Doctoral Degree, and Venia Legendi from Swiss Federal Institute of Technology (ETH), Zürich in 1975, 1980, and 1987 respectively. In 1999 he was given the title of Professor.

Since 1976 he has been working at the ETH on the development of methods for computational electromagnetics and for optimization problems. He has developed the Multiple Multipole Program (MMP), the MaX-1 package, the Generalized Genetic Programming (GGP) code, and various optimization codes. He worked on various applications (electrostatics, EM scattering, antenna, waveguides and waveguide discontinuities, gratings, chiral media, etc.). His current focus is on photonic crystals, microstructured optical fibers, and Scanning Nearfield Optical Microscoes (SNOM). In 1990 he obtained the second prize of the Seymour Cray avard for scientific computing and in 2001 he has been awarded the 2000 Outstanding Journal Paper Award by the Applied Computational Electromagnetics Society. He is member of the Electromagnetics Academy.

Jasmin Smajic was born in Tuzla, Bosnia and Herzegovina, in 1971. He received a Dipl. El.-Ing. degree from Faculty of Electrical Engineering, Tuzla in 1996. Since 1996 he has been working at the Faculty of Electrical Engineering in Tuzla on numerical calculation of electromagnetic field, numerical mathematics and optimization. He got a M.Sc. degree in 1998 from the Faculty of Electrical Engineering and Computing in Zagreb, Croatia, for the analysis of magnetic field in non-linear material. He received a Ph.D. in 2001 from Faculty of Electrical Engineering and Computing in Zagreb, Croatia, for numerical calculation of time-varying field in non-linear material and electrical machine design optimization. Since 2002 he is a postdoctoral research fellow in the Computational Optics group of the Laboratory for Electromagnetic Fields and Microwave Electronics at the ETH Zurich. His current research interest includes numerical field calculation and design optimization of photonic crystal devices.

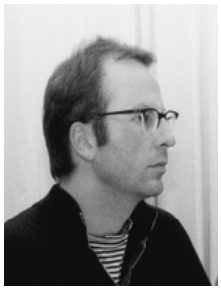

Daniel Erni was born in Lugano, Switzerland, in 1961. He received an El.-Ing. HTL degree from Interkantonales Technikum Rapperswil HTL in 1986, and a Dipl. El.-Ing. degree from Swiss Federal Institute of Technology (ETH), Zürich in 1990, both in electrical engineering. Since 1990 he has been working at the Laboratory for Electromagnetic Fields and Microwave Electronics (ETH) on nonlinear wave propagation, laser diode modeling (multi-section DFB and DBR lasers, VCSELs), computational electromagnetics and on the design of non-periodic optical waveguide gratings e.g. by means of evolutionary algorithms. He got a Ph.D. degree in 1996 for the investigation of non-periodic waveguide gratings and non-periodic coupled cavity laser concepts. His current research interests includes highly multimode optical signal transmission in optical interconnects (i.e. in optical backplanes with extremely large waveguide cross sections) as well as alternative waveguiding concepts for dense integrated optical devices like e.g. photonic crystal devices, couplers and WDM filter structures. In 2001 he has been awarded the 2000 Outstanding Journal Paper Award by the Applied Computational Electromagnetics Society for a contribution on the application of evolutionary optimization algorithms in computational optics. Dr. Erni is the head of the Communication Photonics Group at ETH Zurich (www.photonics.ee.ethz.ch). He is also a member of the Swiss Physical Society (SPS), of the German Physical Society (DPG), of the Optical Society of America (OSA), and of the IEEE

David Karkashadze was born in Tbilisi, Georgia in 1949. He received Master Science in Radio-physics and Quantum Electronics and Candidate of Science Degrees in Radio-physics and Quantum Electronics from Tbilisi State University (TSU), Georgia in 1971 and 1981 respectively.

Since 1971 he has been working at the Department of Physics as a teacher, since 1985 to present General Physics Associate Professor (TSU).

His current research interests include: numerical methods for solution diffraction and wave propagation problems; theoretical and experimental investigation, computer simulation of electrodynamics phenomena; ESD and Transient field calculation; theory and application of wave scattering and propagation in complex (Chiral and Bi-anisotropic) media; development of EM software for engineering.

Revaz Zaridze was born in May 8, 1938, in Georgia, USSR. He received the M.S. and Candidate of Science degrees in radio engineering from Tbilisi State University (TSU), Georgia, in 1962 and 1973, respectively, and the Doctor degree from the Radio-Engineering Institute of the USSR Academy of Sciences, Moscow, USSR, in 1986.

Since 1964, he has taught General Physics course in the Department of Physics, currently is a General Physics Professor. Since 1973 he is Head of the Laboratory of Applied Electrodynamics, TSU, leading the group in researching problems in diffraction and propagation of electromagnetic waves. He developed the numerical method of auxiliary sources for solving the applied problems. 1995 – Member of Management Committee of European Society - COST 243, 261 in area of EMC, Member of IEEE, Chapter Organizer and Chapter Chairman of IEEE Division in Republic of Georgia. His research interests have been in numerical methods for solution diffraction and wave propagation problems, theoretical and experimental investigation of electrodynamics problems, computer simulation of electrodynamics phenomena in multipurpose systems, scattering of EM and acoustic fields from bodies with complex shapes and various surface, field reconstruction and visualization. Also, ESD and transient field calculation, wave propagation in chiral and bianizotropic media, influence of the electromagnetic field on biological object, imaging, tomography, holography, and EMC analysis.

Alexander Bijamov was born in Tbilisi, Georgia in 1978. He received his Bachelor of Physics and Master of Physics degree on the investigation and software creation for the e mobile phones antennas development from the Faculty of Physics at the Tbilisi State University in 1999 and in 2001 correspondingly. Since 1997 he has been working in the Laboratory of Applied Electrodynamics ant the Department of Physics, TSU. He worked on various applications in the field of Applied Electrodynamics and EMC problems, mainly on mobile antenna design. His current research interests include Antenna-with–head interaction modeling and development and simulation of the FPC-based devices. Currently he works on his PhD thesis on Photonic Crystals